

Earthquake Research Western Great Basin

*USGS NEHRP 1998 Technical Report
Contract No. 1434-94-G-2479*

GENE A. ICHINOSE, JOHN G. ANDERSON, and KENNETH D. SMITH[†]

[†] University Nevada Reno Seismological Laboratory
Mackay School of Mines
Mail Stop-174
Reno, NV, 89557-0141
phone (702) 784-4265

Investigations

1. Finished the analysis of stress triggering of aftershocks by the 1994 Double Spring Flat, Nevada, earthquake
2. Finished the seismic analysis of Kean Canyon, Nevada Explosion.

Results *A Test For Static And Dynamic Stress Changes On Triggered Aftershocks Caused By The 1978 Diamond Valley, California And 1994 Double Spring Flat, Nevada Earthquakes*

We studied the 1994 M_w 5.8 Double Spring Flat earthquake sequence in the context of plausible prior stresses and the evolution of Coulomb failure stress, σ_f , as the aftershock sequence evolved (Fig. 1). The timing of the Double Spring Flat earthquake could have been delayed by static stress changes due to the 1978 M 5.2 Diamond Valley earthquake (Somerville et al., 1980). The magnitude of the σ_f decrease, and a time of 16 years for the stresses to reaccumulate between 1978 and 1994, implies a minimum regional stressing rate of 0.013 bars/yr. Aftershocks from the 1994 earthquake migrated south-eastward from the Genoa fault zone towards the Antelope Valley fault zone along a series of conjugate fault pairs (Ichinose et al., 1998a).

We compare static $\Delta\sigma_f$ and dynamic $\Delta\sigma_f$ to aftershock locations and rake angles to possibly determine if nearby aftershocks are more likely triggered by near field pulse or by the passing of seismic waves. The static $\Delta\sigma_f$ and dynamic $\Delta\sigma_f$ was computed for planes of expected failure surrounding the 1994 mainshock plane. The dynamic $\Delta\sigma_f$ is a time series which we chose the peak to peak values for our comparisons. The static $\Delta\sigma_f$ locations are consistent with an increase of σ_f from the 1978 and 1994 mainshocks, if the mechanisms are left-lateral slip on northeast striking planes and normal slip on north-south striking planes dipping east. The conjugate northwest strike-slip plane is also moved toward failure if the mechanisms are right-lateral slip (Fig. 1). The December 1995 aftershock cluster would have also increased σ_f southward along the northern Antelope Valley fault, where three $M > 4$ aftershocks occurred in 1996.

The peak to peak dynamic $\Delta\sigma_f$ was greatest for high angle strike-slip faults and about 1/2 smaller for rakes around -90° (Fig. 2). The dynamic positive $\Delta\sigma_f$ lobes are also occur in the same

location of static positive $\Delta\sigma_f$ lobes. Distance fall-off of aftershocks from the mainshock fault plane are also compared to r^{-3} and r^{-1} models which are characteristics of stress decay for intermediate- and far-field terms. The spatial density of aftershocks that are triggered by static stress changes may, like the stress itself, decay at rates $\geq r^{-3}$, while aftershocks triggered by dynamic stress changes might, like the dynamic strain amplitude, decay as r^{-1} . Eight aftershock sequences including the Double Spring Flat earthquake favor a r^{-1} distance decay, suggesting that dynamic stress changes are an important factor as an aftershock triggering mechanism.

Synthetic dynamic $\Delta\sigma_f$ time histories show radiation patterns similar to the static $\Delta\sigma_f$ and a distance decay of r^{-1} , thereby making it difficult to differentiate either triggering mechanisms by spatial correlation. We did observe larger dynamic σ_f especially at farther distances and others have suggested that transient loads can also advance the time to instabilities using simple spring-slider model (Gomberg et al., 1997), based on Dieterich's (1994) rate- and state-dependent friction constitutive laws. We feel that conditions exist for dynamic stress changes to drive Dieterich's (1994) triggering model by hysteresis motions as well as by discrete stress steps. This may be a plausible mechanism for delayed triggering like remote triggering seen after the 1992 Landers earthquake (Anderson et al., 1994).

For future studies we are interested in how stress concentrations occur in regions of normal fault step-over segments and their correlations to zones of high modern seismicity. The 1978 and 1994 earthquakes between the Genoa and Antelope Valley fault zones provide a good example and we have identified other possible sites in the Western Great Basin to apply this analysis.

Seismic Analysis of an Industrial Accident

On the morning of January 7, 1998, an unfortunate fatal accident occurred at the Kean Canyon chemical plant east of Reno, Nevada. The recently organized US Chemical Safety and Hazard Investigation Board (CSB), with the cooperation of several state agencies, initiated an investigation into the accident with the long range goal of improving the safety at explosive manufacturing facilities. An important aspect of the investigation was determining the chronology of events. John Piatt at the CSB reported that the accident consisted of two explosions that occurred within about 3.5 seconds and were separated horizontally by approximately 250 feet (76.2 meters), along a direction of S33°E. The CSB requested that the Seismological Laboratory independently look into the explosion. Using an high precision cross-correlation method applied to both seismic and air-waves recorded at several seismic stations in northern Nevada, we are able to resolve the relative locations, and azimuth between the sources and the chronology of two explosions.

The difference in moveout of air-waves between the two explosions, measured at several stations, associates the southern site with the second explosion. The separation of explosions, based on an analysis of these air-wave arrivals, at 3 stations is about 73 meters with an uncertainties ranging from ± 7 to 21 meters. We obtained only a single estimate of source separation using P-waves which is 80 meters with a larger uncertainty of ± 78 meters. We did a simultaneous determination of the separation and the azimuth of the explosions which combines the moveout at different stations. The best solution occurs with a separation of 73.2 meters with the second explosion occurring at azimuth of S35°E from the first (Fig. 3). These estimates are well within uncertainties of investigation by the US Chemical Safety and Hazard Investigation Board.

From the relative spectral amplitudes of P- and air-waves, we suggest that explosion B had downward directivity, while A may have been more upwards directed. The corner frequency of the P-waves is much smaller than expected for the physical dimension of the explosions, indicating that

attenuation is exerting a major influence on the P-wave spectrum at high frequency.

The scientific forensic results of this analysis has provided useful information in the US Chemical Safety and Hazard Board's investigation. We confirm that the relative separation of sources can be determined precisely using only a pair of regional seismic stations which can be helpful in investigating accidents. We are encouraged that this approach may also be applied to earthquakes.

References

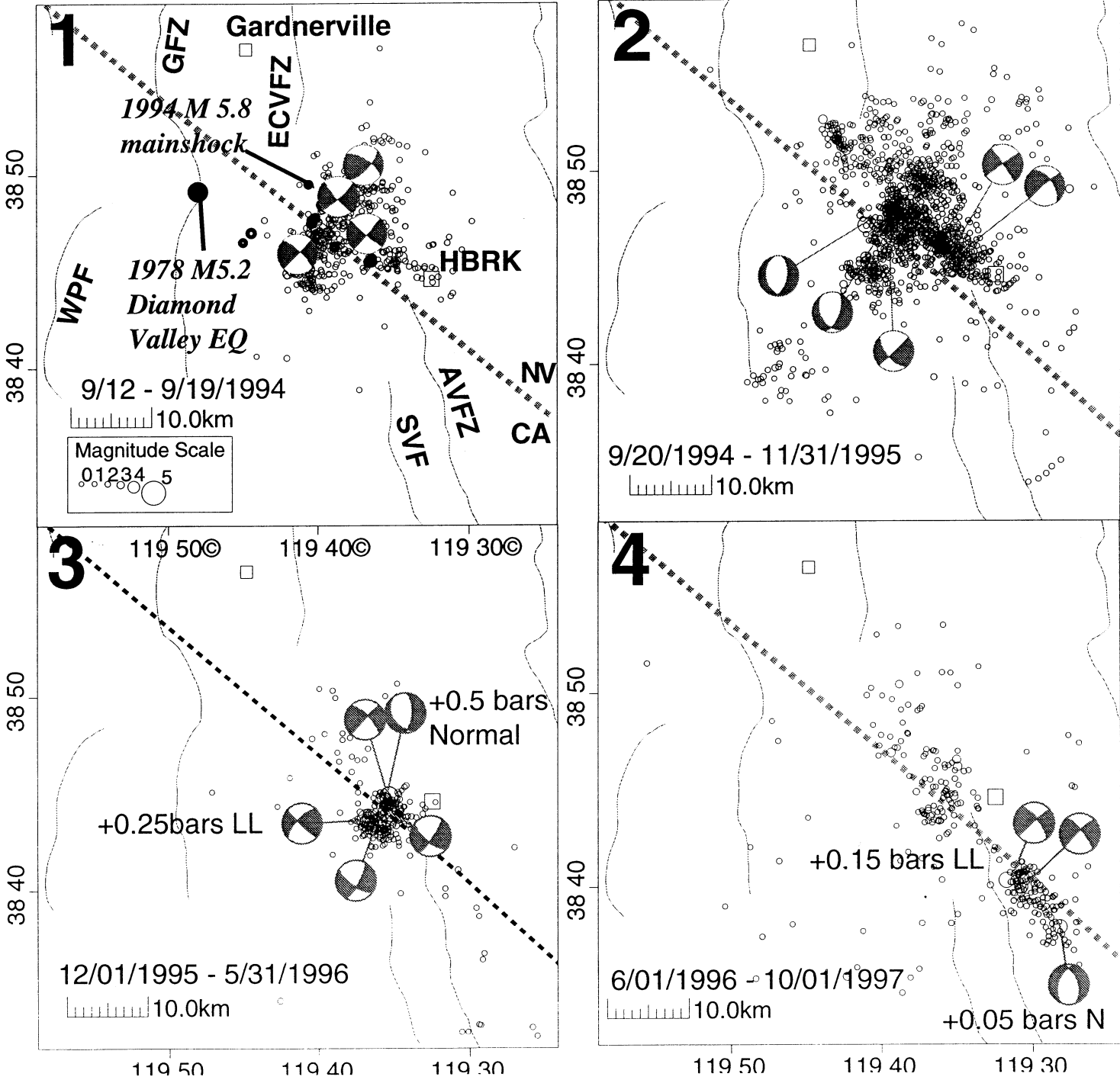
- Anderson, J. G., J. N. Brune, J. N. Louie, Y. Zeng, M. Savage, G. Yu, Q. Chen, and D. dePolo (1994). Seismicity in the western Great Basin apparently triggered by the Landers, California earthquake, 28 June 1992, *Bull. Seism. Soc. Am.*, 84, 863-891.
- Dieterich, J. H. (1994). A constitutive law for rate of earthquake production and its application to earthquake clustering, *J. Geophys. Res.*, 99, 2601-2618.
- Gomberg, J., M. L. Blanpied, and N. M. Beeler (1997). Transient triggering of near and distant earthquakes, *Bull. Seism. Soc. Am.*, 87, 294-309.
- Ichinose, G. A., K. D. Smith, and J. G. Anderson, Moment Tensor inversions of the 1994 to 1996 Double Spring Flat, Nevada Earthquake Sequence and implications for local tectonic models, *Bull. Seismo. Soc. Am.*, In Press, 1998a.

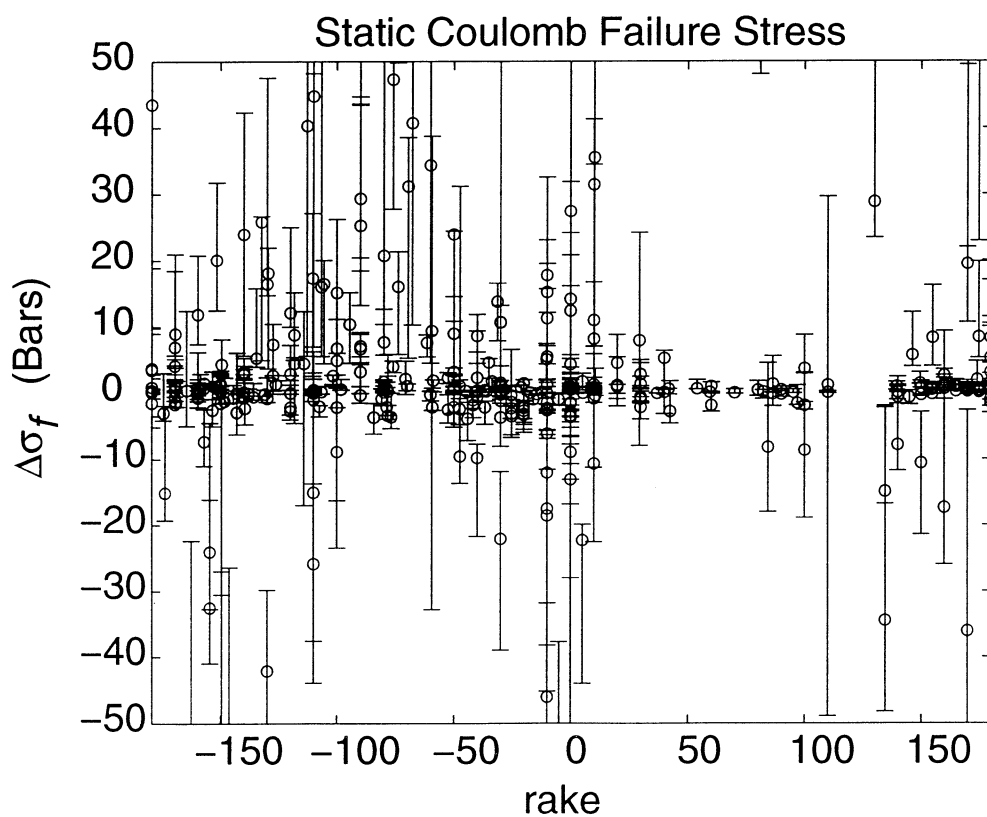
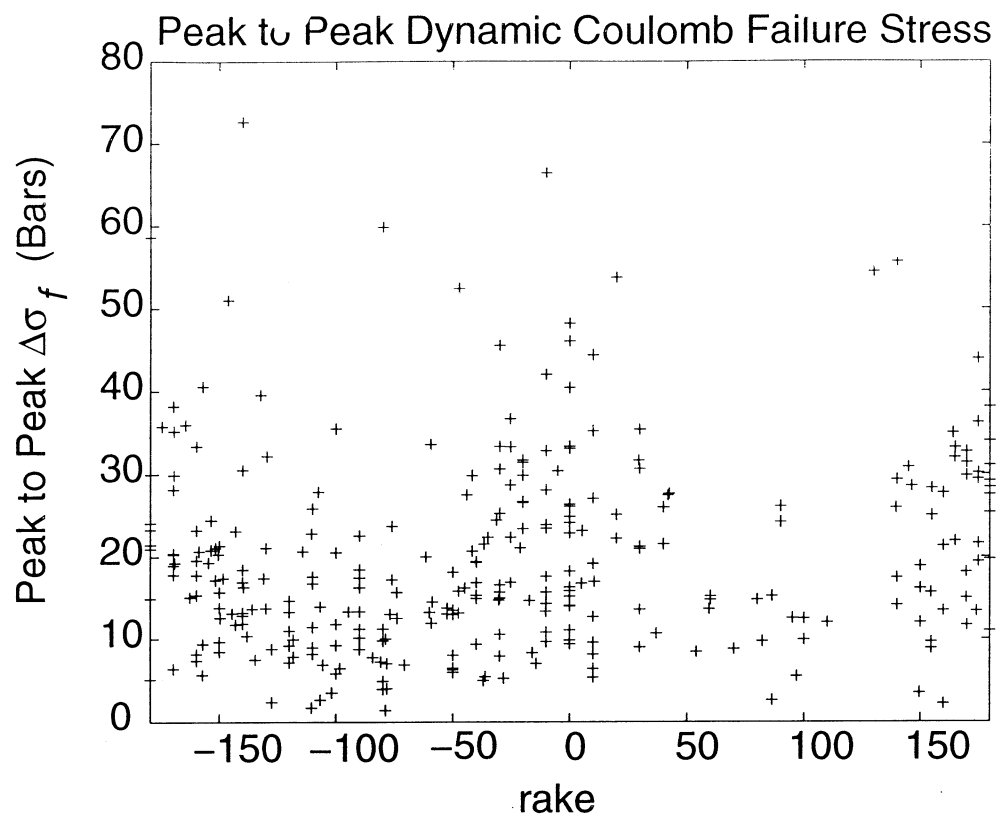
Reports

- Ichinose, G. A., J. G. Anderson, and K. D. Smith, Static stress changes caused by the 1978 Diamond Valley, California and 1994 Double Spring Flat, Nevada earthquakes (abstract), *EOS Transactions, American Geophysical Union*, Vol. 78, 1997.
- Ichinose, G. A., K. D. Smith, and J. G. Anderson, A test for dynamic and static stress changes caused by the 1978 Diamond Valley, California and 1994 Double Spring Flat, Nevada earthquakes, (Submitted to BSSA), 1998b.
- Anderson, J. G., K. D. Smith, and G. A. Ichinose, Seismic analysis of an industrial accident, (Submitted to *Bull. Seismo. Soc. Am.*), 1998c.



Figure 1. Panel 1. shows the aftershocks along a northeast plane in the first week following the 1994 Double Spring Flat earthquake. The $M > 4$ focal mechanisms are also plotted in each corresponding time period. Panel 2. shows that the aftershocks progressed to the north-west striking conjugate fault plane a week after the mainshock. A year after the 1994 mainshock, the activity in Panel 3 shows an alignment along another northwest striking plane near Holbrook Junction (HBRK). The focal mechanisms of five $M > 5$ events in Panel 3 correlate with increases of Coulomb failure stress caused by the 1994 mainshock and its largest aftershock. The Coulomb failure stress was resolved onto left-lateral (LL) and normal (N) faults. Panel 4 shows the further southwestward migration of events toward the Antelope Valley fault in 1996. WPF-Waterhorse Peak, GFZ-Genoa, ECVFZ-Eastern Carson Valley, SVF-Slinkard Valley, AVFZ-Antelope Valley.





The dynamic and static Coulomb failure stress computed from the 1994 Double Spring Flat earthquake. The change in CFS is resolved onto both planes of 113 relocated aftershock focal mechanisms. (a) The peak-to-peak value of the dynamic CFS time series is plotted versus rake angle. (b) The static change in CFS versus is plotted versus rake angle. The error bars in (b) represents the 90% confidence level of rake value.

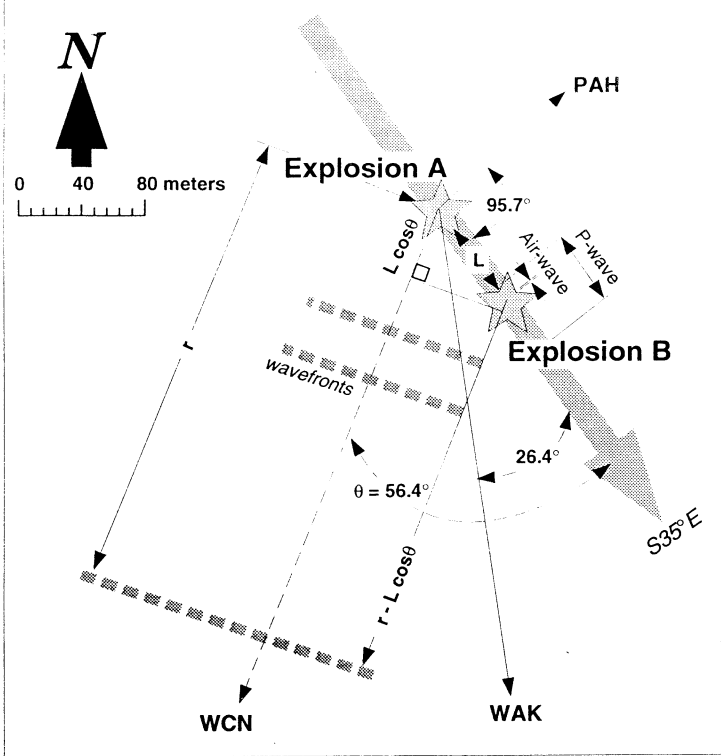


Figure 5. A Schematic map of the explosion site with likely geometry of explosions marked as "stars" and the estimated relative separations shown as uncertainties along azimuth of S35°E. See equation (3) in text for variable definitions. The

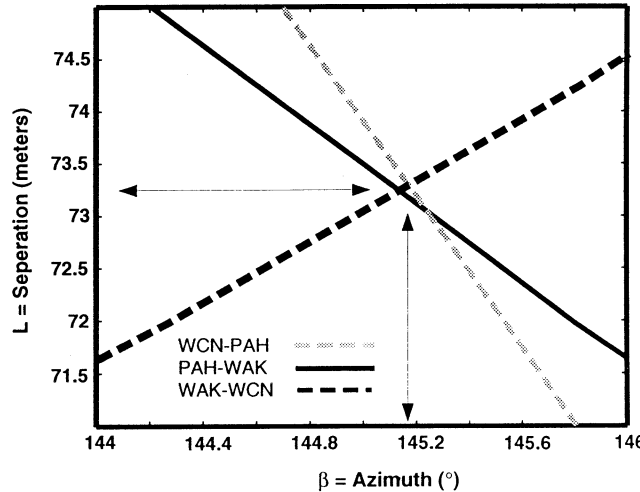
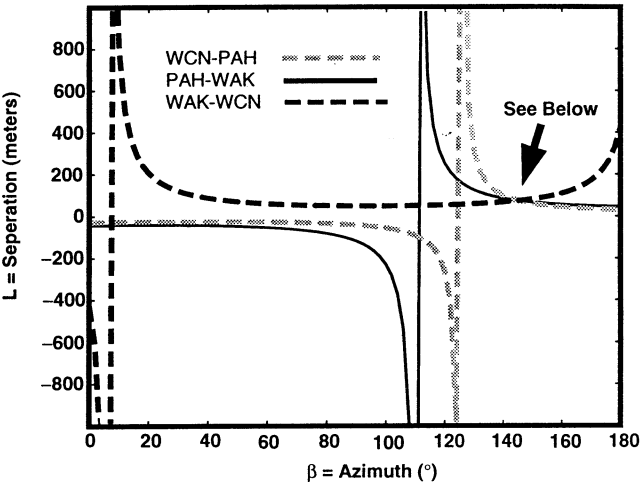


Figure 4. A plot of L, the source separation versus β, the azimuth between sources. The arrows point to the best solution for L and β.